NDT and E International 98 (2018) 155–160

Contents lists available at ScienceDirect

NDT and E International

journal homepage: www.elsevier.com/locate/ndteint

Imaging x70 weld cross-section using electromagnetic testing

Hanyang Xu [a], Jorge Ricardo Salas Avila [a], Fanfu Wu [b], Matthew J. Roy [c], Yuedong Xie [a,*], Frank Zhou [b], Anthony Peyton [a], Wuliang Yin [a]

[a] School of Electrical and Electronic Engineering, University of Manchester, Manchester, M13 9PL, UK
[b] WMG, University of Warwick, Coventry, CV4 7AL, UK
[c] School of Mechanical, Aerospace and Civil Engineering, The University of Manchester, Manchester, M13 9PL, UK

ARTICLE INFO

Keywords:
Welding inspection
Imaging
Non-destructive testing
Electromagnetic
Microstructure

ABSTRACT

Weld inspection is significant in manufacturing to improve productivity and ensure safety. During the welding process, steel microstructures experience complex transformations depending on welding conditions such as heat input, welding speed, component size and temperature, etc. Examining weld microstructures can reveal valuable information on its metallurgical, mechanical and electromagnetic properties. Electromagnetic (EM) testing is of great practical interest to characterise the weld microstructures in a non-destructive and expedient manner. In this paper, an experimental scanning method using a cup-ferrite enclosed T-R sensor has been devised to image the EM properties of a cross-section of an X70 steel submerged arc welding (SAW) specimen. These images show good correlation with the hardness testing and metallurgical information of the specimen. An approximate linear relationship was found between the EM signal and the hardness of the SAW of X70 steel weld. The scanning method can serve as a complementary tool for hardness testing without the need for sophisticated surface preparation.

1. Introduction

WELDING is a widely used fabrication technique in manufacturing industries. In the past decades, considerable efforts have been made to study the metallurgical and mechanical performance of weldments. Hardness testing is one the main techniques used to assess the mechanical performances, as empirical relationships to properties such as tensile strength, yield stress and ductility can be derived [1,2]. In recent years, electromagnetic testing has been increasingly used in welding inspection due to its correlation with the conductivity and permeability of metal weldments and its inherent advantage of being non-destructive and expedient.

Electromagnetic methods have been widely used for metal characterization. Based on Barkhausen effects, linear relationships between stress states and magnetic Barkhausen noises of different ferromagnetic steels was established [3,4,5]. V. Moorthy distinguished four kinds of different microstructures by a U shaped magnetic yoke sensor [6]. Yin developed a method that could determine the conductivity and permeability profile of layered flat conductor with an eddy current sensor [7,8]. The link between general EM sensor output and the distribution of microstructures of ferrite/austenite steel models have been established and experimentally proven [9,10]. EM properties have also been proven to be related to the pearlite percentage and hardness of cast irons by means of eddy current testing (ECT) [11]. Similarly, the relationship between microstructure, hardness and EM properties (conductivity σ and permeability μ) have also been established for a variety of alloys [12,13,14,15]. M Zergoug et al. evaluated the hardness and EM properties of both aluminum and ferromagnetic steels and the results indicated a linear relationship [16]. For welding inspection, T.G. Santos etc. produced an electrical conductivity map of friction stir welding (FSW) joints of thin aluminum alloy plates [17]. The conductivity map showing a clear contour of different zones of weld. However, there are no reports on EM imaging of the weld cross-section of steels, for which both permeability and conductivity affect the outputs of EM sensor.

In the present work, an experimental scanning system and method based on electromagnetic induction has been developed to image the EM properties of a cross-section of an API X70 steel weld specimen with an EM sensor. The images are then compared to the hardness maps of micro-

* Corresponding author.
E-mail addresses: hanyang.xu@postgrad.manchester.ac.uk (H. Xu), jorge.salasavila@postgrad.manchester.ac.uk (J.R. Salas Avila), fanfu.wu@warwick.ac.uk (F. Wu), matthew.roy@manchester.ac.uk (M.J. Roy), yuedong.xie@manchester.ac.uk (Y. Xie), Lei.Zhou@warwick.ac.uk (F. Zhou), A.peyton@manchester.ac.uk (A. Peyton), Wuliang.yin@manchester.ac.uk (W. Yin).

https://doi.org/10.1016/j.ndteint.2018.05.006

Available online 15 May 2018

hardness of the specimen. These EM images show good correlation with hardness map and improve upon the resolution obtained by hardness mapping alone. The size of the specimen can be clearly estimated from the image (with an error of 1.1%) and the shape and size of the weld zones can also be clearly identified. The results indicate that the EM imaging method can serve as a complementary tool for characterizing the mechanical properties of welds with less specimen preparation and measurement time as compared to hardness testing alone.

2. Experimental set-up

2.1. Weld sample description

The base metal (BM) used was API X70 steel rolled to a 26.8 mm × 200 mm × 1 m thick plate. The material was joined by a multi-electrode submerged arc welding (SAW) approach with double 'V' groove. The welding parameters are giving in Table 1. The specimen was the cross-section extracted from the welding joint as shown in Fig. 1. The weld cross-section specimen gives the dimensions of 49 mm traverse (X-axis), 9 mm longitude (Z-axis), and 26.8 mm height (Y-axis) [18]. The surface of the specimen was ground for metallography and hardness testing.

2.2. Hardness and metallography

Hardness investigations on weld cross-section are useful in several ways/scenarios. Many international structural integrity codes specify hardness testing as a quality control measurement, such as ISO15156-1 [19] and ASME BPVC Section IX [20], and there are international standards available which cover the application of singular measurements (e.g. ISO 6507-1 and ASTM E384-10). In addition, the practice of 'mapping' regions with hardness measurements allows one to identify specific metallographic regions in the case of welds. Most importantly, this pertains to the extent of the heat-affected zone (HAZ), where subtle changes in microstructure might not be immediately apparent through standard optical microscopy [21] [22].

During a welding process, the metal microstructure experiences complex transformation which is controlled by adjusting welding parameters such as heat input, welding speed, component size and temperature, etc. [23,24,25]. Depending on these parameters, steels can develop different microstructure phases such as ferrite, austenite, martensite and bainite which all exhibit different hardness values. The specimen employed for this study was mapped using a Vickers indenter and a 1 kg load, with an inter-indent spacing of approximately 1 mm, all hardness values obtained conformed to ASTM E384-10/ISO 6507. Fig. 2 (b) shows the hardness map obtained spanning all regions of the weld. The areas of each of the welds are apparent, including the weld nugget (WN), fusion zone (FZ), and heat affected zone (HAZ) for each weld. Specifically, moving from the weld centerline out to the base metal, the WN has a hardness between 230 and 220 HV1, the FZ is demarked by a drop from 220 to 200 HV1, and the HAZ with a hardness of 200-180 HV1. The microstructure of the weld metal in the WN is fine, acicular ferrite, which then turns to bainite in the HAZ immediately adjacent to the fusion boundary. Regions of high hardness (e.g. the bottom of the WN) are attributed to carbon segregation induced by the back-to-back welding procedure. The obtained microstructure is typical of welds performed in this class of steel.

Table 1
SAW input parameters and weld dimensions.

Weld	Groove depth (mm)	FZ width (mm)	Welding speed (mm/min)	Heat input (kJ/mm)	Arc power (kW)
Backing	9.5	13.4	1600	4.44	188.40
Finishing	11.0	14.0	1370	5.97	136.32

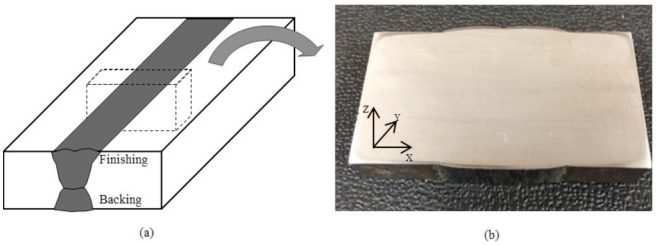

Fig. 1. (a) Schematic of SAW thick plate with finishing and backing bead contour. The steel dimensions are 26.8 mm × 200 mm × 1 m; (b) picture of the cross-section specimen extracted from the SAW API X70 steel as illustrated in (a). The specimen dimensions are 49 mm traverse (X-axis), 9 mm longitude (Z-axis), and 26.8 mm height (Y-axis).

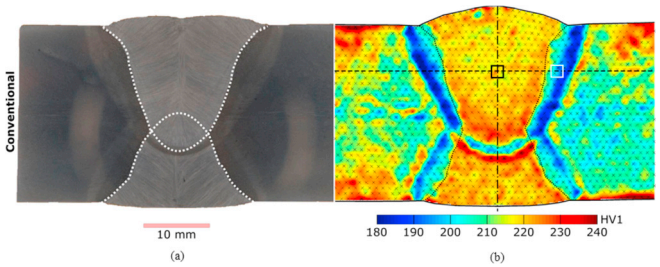

Fig. 2. (a) The macrograph of the weld cross-section; (b) the hardness map of the X70 weld specimen.

Hardness values are obtained by preparing a metallographic surface to a sufficient degree such that indentations can be readily measured. Therefore, increasing level of surface preparation is required to obtain smaller indents, and by virtue, a higher resolution. Micro-hardness testing can, however, produce a reasonable degree of information, albeit with discrete values which must be interpolated over.

2.3. Sensor design

Sensitivity and spatial resolution are of primary importance for sensor specification for material characterisation, in particular for imaging. It is well known that reducing the sensor size can provide a better spatial resolution whereas it also results in a reduction in signal level and sensitivity. A sensor is therefore desired to be as small as possible while meeting the requirements of producing adequate signal.

In this paper, the performance of a cup-ferrite enclosed T-R sensor and a traditional open T-R sensor is evaluated. Their schematics and parameters are introduced in Fig. 3 and Table 2. *Ex* and *Re* denote excitation coil and pickup coil with ferrite cores of a relative μ_i of 2300. For the cup-ferrite sensor, a 10 mm diameter cup-ferrite is added to enclose the T-R sensor with cup wall thickness of 1 mm. The frequency responses of two sensors were measured by the Impedance Analyser (SI1260) as indicated in Fig. 4 (a). The mutual inductance in free space is 70.3 μH for T-R sensor and 17.75 μH for cup-ferrite sensor. Their resonance frequencies are 631 kHz and 794.3 kHz respectively.

The spatial resolution of the sensor was tested with a custom-designed instrument described in section D. The sensor travels above a vertically placed ferrite rod as shown in Fig. 4 (b). The 0.75 mm diameter ferrite rod acts as a point simulation. A 40 kHz excitation frequency was employed to evaluate the lift-off effects.

The spatial resolution of the sensor was defined as the magnitude of the response signal reached half of the peak magnitude as exhibited in Fig. 5. The ratio of resolution to ferrite rod diameter was then used to define the spatial performance. As exhibited in Table 3, the ratio of T-R sensor increases with increased the lift-off while the ratio of cup-ferrite sensor remains almost constant and relatively smaller. These experimental results prove that the ferrite cup is effective at improving the